ORGANOMETALLICS
Article

Organometallics **2009,** *28,* 6585–6592 6585
DOI: 10.1021/om9007357

Scope and Mechanistic Investigations on the Solvent-Controlled Regio- and Stereoselective Formation of Enol Esters from the Ruthenium-Catalyzed Coupling Reaction of Terminal Alkynes and Carboxylic Acids

Chae S. Yi* and Ruili Gao

Department of Chemistry, Marquette University, Milwaukee, Wisconsin 53201-1881

Received August 21, 2009

The ruthenium-hydride complex $(PCy_3)_2(CO)RuHCl$ was found to be a highly effective catalyst for the alkyne-to-carboxylic acid coupling reaction to give synthetically useful enol ester products. A strong solvent effect was observed for the ruthenium catalyst in modulating the activity and selectivity; the coupling reaction in CH_2Cl_2 led to the regioselective formation of *gem*-enol ester products, while the stereoselective formation of (*Z*)-enol esters was obtained in THF. The coupling reaction was found to be strongly inhibited by PCy_3. The coupling reaction of both $PhCO_2H$/$PhC{\equiv}CD$ and $PhCO_2D$/$PhC{\equiv}CH$ led to extensive deuterium incorporation on the vinyl positions of the enol ester products. An opposite Hammett value was observed when the correlation of a series of *para*-substituted *p*-X-$C_6H_4CO_2H$ (X = OMe, CH_3, H, CF_3, CN) with phenylacetylene was examined in $CDCl_3$ ($\rho = +0.30$) and THF ($\rho = -0.68$). Catalytically relevant Ru-carboxylate and -vinylidene-carboxylate complexes, $(PCy_3)_2(CO)(Cl)Ru(\kappa^2\text{-}O_2CC_6H_4\text{-}p\text{-}OMe)$ and $(PCy_3)_2(CO)(Cl)RuC(=CHPh)O_2CC_6H_4\text{-}p\text{-}OMe$, were isolated, and the structure of both complexes was completely established by X-ray crystallography. A detailed mechanism of the coupling reaction involving a rate-limiting C−O bond formation step was proposed on the basis of these kinetic and structural studies. The regioselective formation of the *gem*-enol ester products in CH_2Cl_2 was rationalized by a direct migratory insertion of the terminal alkyne via a Ru-carboxylate species, whereas the stereoselective formation of (*Z*)-enol ester products in THF was explained by invoking a Ru-vinylidene species.

Introduction

Enol esters are a versatile class of precursors for a variety of synthetically important organic transformations such as cycloaddition,[1] asymmetric hydrogenation,[2] C−C bond coupling,[3] and Aldol- and Mannich-type condensation reactions.[4] Since enol esters can also serve as a synthon for aldehydes and ketones, much research effort has been devoted to develop efficient catalytic methods to control both regio- and stereoselectivity in forming substituted enol esters. Notable recent examples on the catalytic synthesis of enol esters include Zr-catalyzed methylalumination of alkynes,[5] Au-catalyzed intramolecular rearrangements of propargylic esters and alcohols,[6] Cu-catalyzed oxidative esterification of aldehydes with β-dicarbonyl compounds,[7] and asymmetric coupling reaction of ketenes with aldehydes by chiral Fe catalysts.[8] From an industrial perspective of increasing synthetic efficiency as well as for reducing waste byproducts, catalytic methods for producing enol esters are highly desired compared to the classical methods that utilize stoichiometric amounts of strong base or toxic Hg salts.[9]

Transition metal-catalyzed alkyne-to-carboxylic acid coupling reactions offer an attractive route to enol esters, but

*Corresponding author. E-mail: chae.yi@marquette.edu.

(1) (a) Nair, V.; Deepthi, A. *Chem. Rev.* **2007**, *107*, 1862–1891. (b) Urabe, H.; Suzuki, D.; Sasaki, M.; Sato, F. *J. Am. Chem. Soc.* **2003**, *125*, 4036–4037. (c) Hara, H.; Hirano, M.; Tanaka, K. *Org. Lett.* **2008**, *10*, 2537–2540.

(2) (a) Brown, J. M. In *Comprehensive Asymmetric Catalysis*; Jacobsen, E. N., Pfalts, A., Yamamoto, H., Eds.; Springer: Berlin, Germany, 1999. (b) Ohkuma, T.; Kitamura, M.; Noyori, R. In *Catalytic Asymmetric Synthesis*; Ojima, I., Ed.; Wiley-VCH: Weinheim, Germany, 2000. (c) Tang, W.; Zhang, X. *Chem. Rev.* **2003**, *103*, 3029–3070.

(3) Trost, B. M.; Toste, F. D.; Pinkerton, A. B. *Chem. Rev.* **2001**, *101*, 2067–2096.

(4) (a) Masuyama, Y.; Kobayashi, Y.; Kurusu, Y. *Chem. Commun.* **1994**, 1123. (b) Yanagisawa, A.; Matsumoto, Y.; Asakawa, K.; Yamamoto, H. *J. Am. Chem. Soc.* **1999**, *121*, 892–893. (c) Karlsson, S.; Högberg, H. E. *Tetrahedron: Asymmetry* **2001**, *12*, 1977–1982. (d) Isambert, N.; Cruz, M.; Arévalo, M. J.; Gómez, E.; Lavilla, R. *Org. Lett.* **2007**, *9*, 4199–4202. (e) Clarke, P. A.; Zaytsev, A. V.; Morgan, T. W.; Whitwood, A. C.; Wilson, C. *Org. Lett.* **2008**, *10*, 2877–2880.

(5) DeBergh, J. R.; Spivey, K. M.; Ready, J. M. *J. Am. Chem. Soc.* **2008**, *130*, 7828–7829.

(6) (a) Wang, S.; Zhang, L. *J. Am. Chem. Soc.* **2006**, *128*, 8414–8415. (b) Wang, S.; Zhang, L. *Org. Lett.* **2006**, *8*, 4585–4587. (c) De Brabander, J. K.; Liu, B.; Qian, M. *Org. Lett.* **2008**, *10*, 2533–2536. (d) Peng, Y.; Cui, L.; Zhang, G.; Zhang, L. *J. Am. Chem. Soc.* **2009**, *131*, 5062–5063.

(7) Yoo, W. -J.; Li, C.-J. *J. Org. Chem.* **2006**, *71*, 6266–6268.

(8) Schaefer, C.; Fu, G. C. *Angew. Chem., Int. Ed.* **2005**, *44*, 4606–4608.

(9) (a) House, H. O. *Modern Synthetic Reactions*, 2nd Ed.; Benjamin/Cummings: Menlo Park, CA, 1972. (b) Smith, M. B.; March, J. *Advanced Organic Chemistry*, 5th ed.; Wiley: New York, 2001.

Published on Web 10/30/2009

their synthetic potential has not been fully exploited in part because the catalytic method typically produces a mixture of *gem*- and (*E*)/(*Z*)-enol ester products.[10] Considerable research has been devoted to control both regio- and stereoselectivity of the enol ester products by modulating the steric and electronic nature of the metal catalysts. Generally, late transition metal catalysts have been found to be effective for producing a mixture of (*E*)- and (*Z*)-enol esters from anti-Markovnikov addition of carboxylic acids to terminal alkynes over *gem*-enol ester products,[10,11] though the regioselective formation of *gem*-enol esters has been achieved by using Ru and Rh catalysts.[12] Dixneuf and co-workers elegantly showed the relationship between steric environment of the ruthenium-phosphine catalysts and the stereoselective formation of the (*Z*)-enol esters.[13] In a subsequent study, the same authors reported a regioselective 2:1 alkyne-to-carboxylic acid coupling reaction to form the dienyl esters by using the Cp*Ru(COD)Cl catalyst, in which a ruthenacyclopentadiene complex was proposed as the key intermediate species for the coupling reaction.[14] Both intra- and intermolecular versions of the catalytic alkyne-to-carboxylic coupling methods have been successfully applied to the synthesis of complex organic molecules.[15] Despite considerable synthetic and mechanistic progress, however, neither the nature of reactive intermediate species nor controlling factors for the formation of *gem*- vs (*E*)/(*Z*)-enol esters have been clearly established.

We previously reported that the coordinatively unsaturated ruthenium-hydride complex $(PCy_3)_2(CO)RuHCl$ (**1**) is a highly effective catalyst for the coupling reactions of alkenes and alkynes.[16] Both ruthenium-acetylide and -vinylidene complexes have been found to be the key species for these coupling reactions.[17] As part of ongoing efforts to extend synthetic utility of the ruthenium-catalyzed alkyne coupling reactions, we have been exploring the catalytic activity of the ruthenium-hydride complexes toward the coupling reactions of alkynes with heteroatom substrates. In this article, we report a detailed scope and mechanistic study of the ruthenium-catalyzed alkyne-to-carboxylic acid coupling reaction, which provides new insights in mediating solvent-controlled regio- and stereoselective formation of the enol ester products.

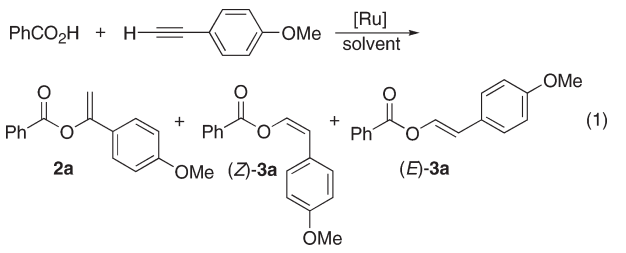

Results and Discussion

Catalyst Survey and Reaction Scope. The catalytic activity of selected ruthenium complexes was initially screened for the coupling reaction of benzoic acid and 4-ethynylanisole (eq 1). Among the selected ruthenium catalysts, complex **1** was found to exhibit uniquely high catalytic activity and selectivity in giving the *gem*-enol ester product **2a** within 5 h at 95 °C in CH_2Cl_2 (Table 1). Both $Ru_3(CO)_{12}$ and $Cp^*Ru(PPh_3)_2Cl$ showed significant activity, but suffered from low selectivity in forming the coupling products. The catalyst Cp*Ru(COD)Cl, on the other hand, produced a mixture of 1:1 and 1:2 coupling products, which is in line with the previously reported results on the formation of dienyl ester products.[14]

Next, the solvent effect on the activity and selectivity patterns of the catalyst was examined for the coupling reaction of benzoic acid and 4-ethynylanisole (Table 2). A remarkably strong solvent influence on the ruthenium catalyst **1** was observed in modulating the formation of the enol ester products. Thus, the coupling reaction in relatively nonpolar and noncoordinating solvents tended to favor the formation of geminal coupling product **2a** over (*E*)- and (*Z*)-**3a**, of which CH_2Cl_2 was found to be the best in producing the geminal product **2a** among these solvents (entry 4). In contrast, among polar coordinating solvents, which tended to favor the formation of (*Z*)-enol ester product (*Z*)-**3a**, THF was found to be the most selective in giving (*Z*)-**3a** (entry 10). It should be emphasized that the formation of 1:2 coupling products was not observed from the coupling reaction catalyzed by **1**. Other ruthenium catalysts such as $Ru_3(CO)_{12}$, $Cp^*Ru(PPh_3)_2Cl$, and Cp*Ru(COD)Cl surveyed in Table 1 did not exhibit a similar degree of solvent control in forming the coupling products.

It is imperative to briefly mention the recent advances in using solvents with different polarity and coordinating ability to control the product selectivity. Coordinatively unsaturated transition metal complexes have been found to be particularly sensitive to the nature of solvents in mediating unreactive bond activation reactions.[18−20] For example,

(10) Selected review articles: (a) Bruneau, C.; Dixneuf, P. H. *Acc. Chem. Res*. **1999**, *32*, 311–323. (b) Drozdak, R.; Allaert, B.; Ledoux, N.; Dragutan, I.; Dragutan, V.; Verpoort, F. *Adv. Synth. Catal*. **2005**, *347*, 1721–1743.

(11) (a) Bianchini, C.; Meli, A.; Peruzzini, M.; Zanobini, F.; Bruneau, C.; Dixneuf, P. H. *Organometallics* **1990**, *9*, 1155–1160. (b) Doucet, H.; Höfer, J.; Bruneau, C.; Dixneuf, P. H. *Chem. Commun*. **1993**, 850–851. (c) Melis, K.; Opstal, T.; Verpoort, F. *Eur. J. Org. Chem*. **2002**, 3779–3784. (d) Nakagawa, H.; Okimoto, Y.; Sakaguchi, S.; Ishii, Y. *Tetrahedron Lett*. **2003**, *44*, 103–106. (e) Hua, R.; Tian, X. *J. Org. Chem*. **2004**, *69*, 5782–5784. (f) Doherty, S.; Knight, J. G.; Rath, R. K.; Clegg, W.; Harrington, R. W.; Newman, C. R.; Campbell, R.; Amin, H. *Organometallics* **2005**, *24*, 2633–2644.

(12) (a) Mitsudo, T.; Hori, Y.; Yamakawa, Y.; Watanabe, Y. *J. Org. Chem*. **1987**, *52*, 2230–2239. (b) Ho, J. H. H.; Black, D. S.; Messerle, B. A.; Clegg, J. K.; Turner, P. *Organometallics* **2006**, *25*, 5800–5810.

(13) Doucet, H.; Martin-Vaca, B.; Bruneau, C.; Dixneuf, P. H. *J. Org. Chem*. **1995**, *60*, 7247–7255.

(14) Le Paih, J.; Monnier, F.; Dérien, S.; Dixneuf, P. H.; Clot, E.; Eisenstein, O. *J. Am. Chem. Soc*. **2003**, *125*, 11964–11975.

(15) (a) Cherry, K.; Parrain, J.-L.; Thibonnet, J.; Duchêne, A.; Abarbri, M. *J. Org. Chem*. **2005**, *70*, 6669–6675. (b) Wang, Y.; Burton, D. J. *J. Org. Chem*. **2006**, *71*, 3859–3862. (c) Ueura, K.; Satoh, T.; Miura, M. *Org. Lett*. **2007**, *9*, 1407–1409. (d) Kim, H.; Goble, S. D.; Lee, C. *J. Am. Chem. Soc*. **2007**, *129*, 1030–1031.

(16) (a) Yi, C. S.; He, Z.; Lee, D. W. *Organometallics* **2001**, *20*, 802–804. (b) Yi, C. S.; Yun, S. Y.; Guzei, I. A. *Organometallics* **2004**, *23*, 5392–5395. (c) Yi, C. S.; Yun, S. Y. *Org. Lett*. **2005**, *7*, 2181–2183.

(17) (a) Yi, C. S.; Liu, N. *Synlett* **1999**, 281−287, and references therein. (b) Yi, C. S.; Yun, S. Y.; Guzei, I. A. *J. Am. Chem. Soc*. **2005**, *127*, 5782–5783.

(18) (a) Rybtchinski, B.; Milstein, D. *J. Am. Chem. Soc*. **1999**, *121*, 4528–4529. (b) Feller, M.; Iron, M. A.; Shimon, L. J. W.; Diskin-Posner, Y.; Leitus, G.; Milstein, D. *J. Am. Chem. Soc*. **2008**, *130*, 14374–14375.

(19) Swartz, B. D.; Reinartz, N. M.; Brennessel, W. W.; Garca, J. J.; Jones, W. D. *J. Am. Chem. Soc*. **2008**, *130*, 8548–8554.

(20) (a) Grimster, N. P.; Gauntlett, C.; Godfrey, C. R. A.; Gaunt, M. J. *Angew. Chem., Int. Ed*. **2005**, *44*, 3125–3129. (b) Ranu, B. C.; Chattopadhyay, K.; Adak, L. *Org. Lett*. **2007**, *9*, 4595–4598. (c) Cheng, J.-S.; Wei, G.-F.; Huang, S.-W.; Zhao, J.; Jiang, H.-F. *J. Mol. Catal*. **2007**, *263*, 169–174. (d) Zotto, A. D.; Prat, F. I.; Baratta, W.; Zangrando, E.; Rigo, P. *Inorg. Chim. Acta* **2009**, *362*, 97–104.

Table 1. Catalyst Survey on the Coupling Reaction of Benzoic Acid and 4-Ethynylanisole[a]

entry	catalyst	yield (%)[b]	**2a**:(*Z*)-**3a**:(*E*)-**3a**
1	$(PCy_3)_2(CO)RuHCl$ (**1**)	> 95	100:0:0
2	$(PPh_3)_3(CO)RuH_2$	0	
3	$(PPh_3)_3RuCl_2$	0	
4	$(PPh_3)_3RuHCl$	0	
5	$RuCl_3 \cdot 3H_2O$	0	
6	$[RuCl_2(COD)]_x$	0	
7	$Ru_3(CO)_{12}$	90	8:17:75
8	$Cp^*Ru(PPh_3)_2Cl$	50	15:50:35
9	$Cp^*Ru(COD)Cl$	60	22:78[c]

[a] Reaction conditions: benzoic acid (0.10 mmol), 4-ethynylanisole (0.15 mmol), catalyst (2 mol %), CH_2Cl_2 (2 mL), 95 °C, 8 h. [b] GC yields based on benzoic acid. [c] Ratio of **2a** and 1:2 coupling products.

Table 2. Solvent Effect on the Coupling Reaction of Benzoic Acid and 4-Ethynylanisole Catalyzed by 1[a]

entry	solvent	**2a**:(*Z*)-**3a**:(*E*)-**3a**	yield (%)[b]
1	benzene	51:40:9	80
2	toluene	68:26:6	70
3	*n*-hexane	71:18:11	75
4	CH_2Cl_2	99:1:0	> 99
5	Et_2O	13:20:67	60
6	CH_3CN	33:55:13	55
7	DME	5:74:21	50
8	DMSO	2:48:50	53
9	H_2O	3:44:53	73
10	THF	0:100:0	> 99

[a] Reaction conditions: benzoic acid (0.10 mmol), 4-ethynylanisole (0.15 mmol), **1** (14 mg, 2 mol %), solvent (2 mL), 95 °C, 8 h. [b] GC yields based on benzoic acid.

Milstein discovered a remarkable solvent effect of the pincer-ligated (PCP)Rh complexes in directing C−H vs C−C bond and C−I vs C−CN bond activation reactions.[18] Jones investigated the similar solvent control effects in C−C vs C−H bond cleavage reactions of alkenyl nitriles by using well-defined Ni-diphosphine complexes.[19] The regioselectivity of a number of synthetically useful catalytic coupling reactions of alkenes and alkynes, such as Heck-type and allylic substitution reactions, has also been successfully controlled by using different solvents.[20]

The scope of the coupling reaction was surveyed in both CH_2Cl_2 and THF by using the catalyst **1** (Table 3). An excellent degree of solvent control was observed for the coupling reaction of terminal alkynes with carboxylic acids in facilitating regio- and stereoselective formation of the enol ester products. Thus, the coupling reaction in CH_2Cl_2 led to the exclusive formation of the *gem*-enol ester product **2** for both aliphatic and aryl-substituted terminal alkynes. In contrast, the coupling reaction for aryl-substituted alkynes in THF predominantly gave the (*Z*)-enol ester products (*Z*)-**3**. The electronic nature of the alkynes was found to be an important factor in dictating regioselective product formation, since *gem*-enol ester product **2** was formed predominantly with the aliphatic terminal alkynes, even when the reaction was performed in THF (entries 17−19, 32, 34). In all cases, a relatively low catalyst loading (1−2 mol %) was used for the coupling reaction, and the enol ester products were readily isolated in high yields after a simple column chromatography on silica gel.

To further demonstrate the synthetic efficacy of the ruthenium catalyst **1**, we next examined the coupling reaction of carboxylic acids with both propargylic alcohols and diynes (Table 4). The catalyst **1** was found to catalyze the coupling

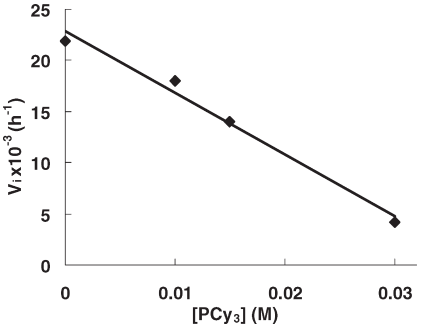

Figure 1. Plot of the initial rate (v_i) vs [PCy_3] for the coupling reaction of benzoic acid and phenylacetylene.

Scheme 1

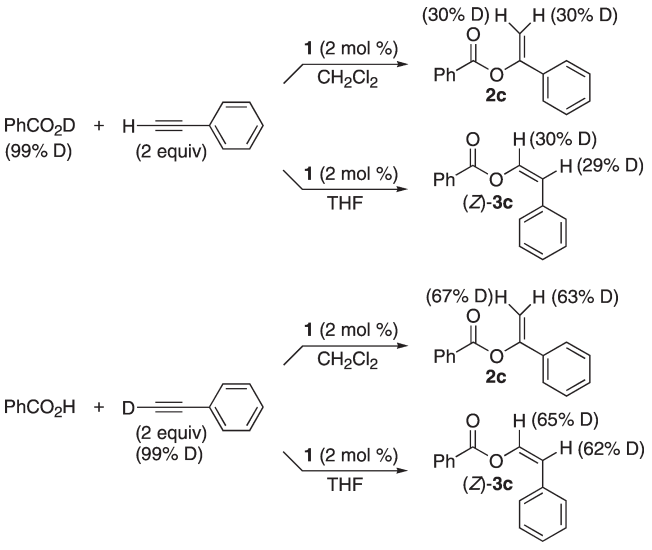

reaction of carboxylic acids with propargylic alcohols to give the acetomethyl ester products **4** in high yields. In these cases, exclusive formation of the ketone product was formed from the Markovnikov-selective hydration of the alkynes. Such Markovnikov selectivity has been generally preferred for the hydration of terminal alkynes,[21] although anti-Markovnikov selective hydration of alkynes has been achieved more recently by using late transition metal catalysts.[22] The analogous coupling reaction with an aryl-substituted diyne 1,4-diethynylbenzene in CH_2Cl_2 predictably yielded the corresponding *gem*-dienol diester product **5a** (entry 8), while a mixture of *gem*-, (*E*)-, and (*Z*)-dienol diester products was formed in THF (*gem*:*E*:*Z* = 18:32:50, 91% combined yield). In contrast, an aliphatic diyne produced *gem*-dienol diester **5b** exclusively in both CH_2Cl_2 and THF (entry 9).

Mechanistic Study: Phosphine Inhibition Study. The following experiments were performed to probe the factors influencing the formation of the enol ester products. First, the phosphine inhibition kinetics was measured from the

(21) (a) Bruce, M. I. *Chem. Rev.* **1991**, *91*, 197–257. (b) Tani, K.; Kataoka, Y. In *Catalytic Heterofunctionalization*; Togni, A., Grützmacher, H., Eds.; VCH-Wiley: Weinheim, 2001; pp 199−207. (c) Bruneau, C.; Dixneuf, P. H. *Angew. Chem., Int. Ed.* **2006**, *45*, 2176–2203.

(22) (a) Grotjahn, D. B.; Incarvito, C. D.; Rheingold, A. L. *Angew. Chem., Int. Ed.* **2001**, *40*, 3884–3887. (b) Tokunaga, M.; Suzuki, T.; Koga, N.; Fukushima, T.; Horiuchi, A.; Wakatsuki, Y. *J. Am. Chem. Soc.* **2001**, *123*, 11917–11924. (c) Grotjahn, D. B.; Lev, D. A. *J. Am. Chem. Soc.* **2004**, *126*, 12232–12233. (d) Labonne, A.; Kribber, T.; Hintermann, L. *Org. Lett.* **2006**, *8*, 5853–5856.

Table 3. Alkyne-to-Carboxylic Acid Coupling Reaction[a]

entry	acid	alkyne	solvent	product ratio (**2**:(*Z*)-**3**:(*E*)-**3**)		yd (%)[b]
1	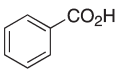	H—≡—C_6H_4-*p*-R	CH_2Cl_2	R = OMe	**2a**:(*Z*)-**3a**:(*E*)-**3a** = 100:0:0	91
2				R = Me	**2b**:(*Z*)-**3b**:(*E*)-**3b** = 100:0:0	87
3				R = H	**2c**:(*Z*)-**3c**:(*E*)-**3c** = 100:0:0	98
4				R = Br	**2d**:(*Z*)-**3d**:(*E*)-**3d** = 100:0:0	89
5				R = CF_3	**2e**:(*Z*)-**3e**:(*E*)-**3e** = 100:0:0	90
6				R = F	**2f**:(*Z*)-**3f**:(*E*)-**3f** = 100:0:0	87
7	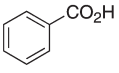	H—≡—C_6H_4-*p*-R	THF	R = OMe	**2a**:(*Z*)-**3a**:(*E*)-**3a** = 0:100:0	95
8				R = Me	**2b**:(*Z*)-**3b**:(*E*)-**3b** = 0:86:14	90
9				R = H	**2c**:(*Z*)-**3c**:(*E*)-**3c** = 0:87:13	98
10				R = Br	**2d**:(*Z*)-**3d**:(*E*)-**3d** = 0:94:6	89
11				R = CF_3	**2e**:(*Z*)-**3e**:(*E*)-**3e** = 0:93:7	90
12				R = F	**2f**:(*Z*)-**3f**:(*E*)-**3f** = 0:90:10	87
13	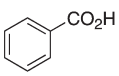	1-hexyne	CH_2Cl_2		**2g**:(*Z*)-**3g**:(*E*)-**3g** = 100:0:0	97
14		$HCCCH_2Ph$			**2h**:(*Z*)-**3h**:(*E*)-**3h** = 100:0:0	96
15		3-methyl-3-buten-1-yne			**2i**:(*Z*)-**3i**:(*E*)-**3i** = 100:0:0	97
16		2-ethynyl-6-methoxynaphthalene			**2j**:(*Z*)-**3j**:(*E*)-**3j** = 100:0:0	87
17	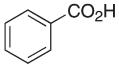	1-hexyne	THF		**2g**:(*Z*)-**3g**:(*E*)-**3g** = 100:0:0	97
18		$HCCCH_2Ph$			**2h**:(*Z*)-**3h**:(*E*)-**3h** = 100:0:0	96
19		3-methyl-3-buten-1-yne			**2i**:(*Z*)-**3i**:(*E*)-**3i** = 100:0:0	97
20		2-ethynyl-6-methoxynaphthalene			**2j**:(*Z*)-**3j**:(*E*)-**3j** = 0:100:0	89
21	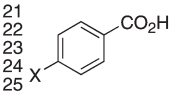	H—≡—Ph	CH_2Cl_2	X = OMe	**2k**:(*Z*)-**3k**:(*E*)-**3k** = 100:0:0	83
22				X = Me	**2l**:(*Z*)-**3l**:(*E*)-**3l** = 100:0:0	90
23				X = Br	**2m**:(*Z*)-**3m**:(*E*)-**3m** = 100:0:0	68
24				X = CN	**2n**:(*Z*)-**3n**:(*E*)-**3n** = 100:0:0	89
25				X = CF_3	**2o**:(*Z*)-**3o**:(*E*)-**3o** = 100:0:0	90
26	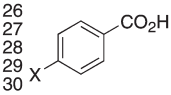	H—≡—Ph	THF	X = OMe	**2k**:(*Z*)-**3k**:(*E*)-**3k** = 0:90:10	95
27				X = Me	**2l**:(*Z*)-**3l**:(*E*)-**3l** = 0:90:10	93
28				X = Br	**2m**:(*Z*)-**3m**:(*E*)-**3m** = 0:92:8	90
29				X = CN	**2n**:(*Z*)-**3n**:(*E*)-**3n** = 3:92:5	83
30				X = CF_3	**2o**:(*Z*)-**3o**:(*E*)-**3o** = 8:81:11	85
31	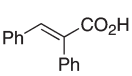	H—≡—Ph	CH_2Cl_2		**2p**:(*Z*)-**3p**:(*E*)-**3p** = 100:0:0	90
32		1-hexyne			**2q**:(*Z*)-**3q**:(*E*)-**3q** = 100:0:0	93
33		H—≡—Ph	THF		**2p**:(*Z*)-**3p**:(*E*)-**3p** = 3:92:5	97
34		1-hexyne			**2q**:(*Z*)-**3q**:(*E*)-**3q** = 100:0:0	96
35	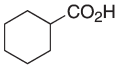	H—≡—Ph	CH_2Cl_2		**2r**:(*Z*)-**3r**:(*E*)-**3r** = 88:12:0	90
36			THF		**2r**:(*Z*)-**3r**:(*E*)-**3r** = 0:93:7	93
37	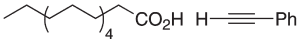		CH_2Cl_2		**2s**:(*Z*)-**3s**:(*E*)-**3s** = 89:11:0	91
38			THF		**2s**:(*Z*)-**3s**:(*E*)-**3s** = 0:90:10	91

[a] Reaction conditions: acid (1.0 mmol), alkyne (2.0 mmol), **1** (14 mg, 2 mol %), solvent (2−3 mL), 90−95 °C, 8−12 h. [b] Isolated yield.

coupling reaction of benzoic acid and phenylacetylene in the presence of the catalyst **1** (2 mol %). The plot of the initial rate (v_i), which was estimated from a first-order plot of *ln*[product] vs reaction time, as a function of [PCy_3] showed that the rate is inversely dependent on added [PCy_3] (Figure 1). The addition of PCy_3 (10−30 mM, 2.5−7.5 mol %) to the reaction mixture under otherwise similar conditions led to a steady decrease from $k_{obs} = 1.8 \times 10^{-2}$ h^{-1} (without added PCy_3) to 4.0×10^{-3} h^{-1} (30 mM of PCy_3). These results indicate that the active Ru catalyst is formed by a reversible dissociation of the phosphine ligand.

Deuterium Labeling Study. The treatment of $PhCO_2D$ with PhC≡CH (2.0 equiv) and **1** (2 mol %) in CH_2Cl_2 at 95 °C yielded the *gem*-enol ester product **2c** with ca. 30% D on both vinyl positions, as determined by ^1H and ^2H NMR (Scheme 1). The analogous reaction in THF also formed the product (*Z*)-**3c** with a similar amount of deuterium on the vinyl positions. Conversely, the reaction of $PhCO_2H$ with PhC≡CD (2 equiv) in CH_2Cl_2 and in THF formed the products **2c** and (*Z*)-**3c**, respectively, with nearly equal amounts of the deuterium (62−67%) on the vinyl positions. In a control experiment, the treatment of $PhCO_2D$ with PhC≡CH (2.0 equiv) in the presence of **1** (2 mol %) led to almost complete H/D exchange within 10 min at 95 °C prior to the product formation. The ruthenium catalyst was found to be essential for the H/D exchange reaction, since no significant H/D exchange between $PhCO_2D$ and PhC≡CH occurred in the absence of **1** under otherwise similar conditions. These results indicate that the H/D exchange between the acid and alkynyl hydrogens is rapid and reversible and that neither the alkynyl C−H bond nor the carboxylic acid O−H bond activation step is a rate-limiting step of the coupling reaction.

Hammett Study. To discern the electronic effects on the product formation, the Hammett ρ values were measured for the coupling reaction in both $CDCl_3$ and THF. Thus, the correlation of relative rates with σ_p for a series of *para*-substituted benzoic acids *p*-X-$C_6H_4CO_2H$ (X = OMe, CH_3, H, CF_3, CN) with phenylacetylene in the presence **1** (2 mol %) at 95 °C led to the opposing trend between the reaction in $CDCl_3$ ($\rho = +0.30$) and in THF ($\rho = -0.68$) (Figure 2).[9b] An analogous correlation of the reaction rates of benzoic acid with a series of *para*-substituted alkynes *p*-Y-$C_6H_4C{\equiv}CH$ (Y = OMe, CH_3, H, F, CF_3) also resulted in the opposite slope between two solvents ($\rho = -0.57$ in $CDCl_3$ vs $\rho = +0.33$ in THF) (Figure 3).

The opposite Hammett ρ value indicates a different mechanistic pathway between the coupling reaction in $CDCl_3$ and in THF. The positive ρ value observed from the correlation of *para*-substituted benzoic acids *p*-X-$C_6H_4CO_2H$ in $CDCl_3$ matches well with a direct migratory insertion of the carboxylate group to a coordinated terminal alkyne, which is dictated by the nucleophilicity of a developing negative charge on the carboxylic oxygen. On the other hand, a negative ρ value obtained from the reaction in THF indicates considerable cationic character buildup on the

Table 4. Coupling Reaction of Carboxylic Acids with Propargylic Alcohols and Diynes[a]

entry	acid	alkyne	product(s)	yield (%)[b]
1	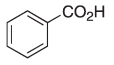	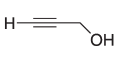	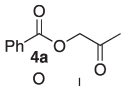	98
2		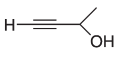	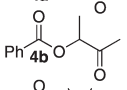	95
3		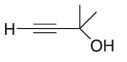	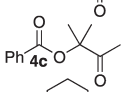	97
4			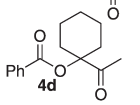	90
5	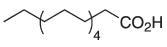	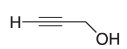	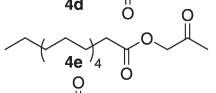	89
6	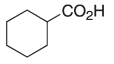	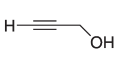	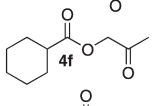	83
7	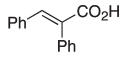	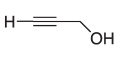	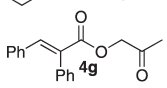	85
8[c]	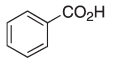	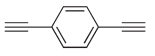	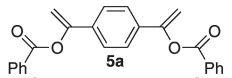	90
9[c]		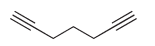	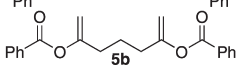	94

[a] Reaction conditions: carboxylic acid (1.0 mmol), alkyne (2.0 mmol), **1** (14 mg, 2 mol %), CH_2Cl_2 (2−3 mL), 90−95 °C, 8−12 h. [b]Isolated yield. [c]48 h of the reaction time.

transition state, and this can be explained via the formation of the Ru-vinylidene species, wherein electrophilic character of the α-vinylidene carbon has been well established.[10a,21a] The analogous opposite trend from the correlation of the alkynes *p*-Y-$C_6H_4C{\equiv}CH$ can similarly be rationalized in terms of developing a positive charge on the alkynyl carbon. Thus, a negative ρ value in $CDCl_3$ is consistent with the positive charge buildup on the *internal* alkynyl carbon, while a positive ρ value in THF suggests an electrophilic character on the *terminal* alkynyl carbon. Once again, the latter case is consistent with the formation of a Ru-vinylidene species and the addition of the carboxylate group to the electrophilic α-vinylidene carbon in the transition state.

Catalytically Relevant Ruthenium-Carboxylate and -Vinylidene-Carboxylate Complexes. A catalytically relevant ruthenium-carboxylate complex was successfully isolated from the reaction of **1** with a carboxylic acid. For example, the treatment of **1** (72 mg, 0.10 mmol) with *p*-OMe-$C_6H_4CO_2H$ (16 mg, 0.11 mmol) in CH_2Cl_2 (2 mL) at room temperature for 10 h led to the clean formation of the ruthenium-carboxylate complex **6**, which was isolated in 87% yield after recrystallization in CH_2Cl_2/hexanes. The complex **6** exhibited two sets of aryl protons at δ 7.88 (d, J = 8.7 Hz) and 6.89 (d, J = 8.7 Hz) in the ^{1}H NMR, as well as two carbonyl peaks at δ 208.8 (t, J_{CP} = 13.3 Hz, CO) and 179.0 (s, CO_2) in the $^{13}C\{^1H\}$ NMR. A single phosphine peak at δ 28.7 was also observed by the $^{31}P\{^1H\}$ NMR. The structure of **6** was further established by X-ray crystallography (Figure 4). The molecular structure showed a pseudooctahedral geometry around the ruthenium center with trans phosphine and cis CO and Cl^- ligand arrangements. A slightly larger than 90° bond angle between CO and Cl^- ligands (96.4°) may be due to a κ^2-bonding mode of the carboxylate ligand.

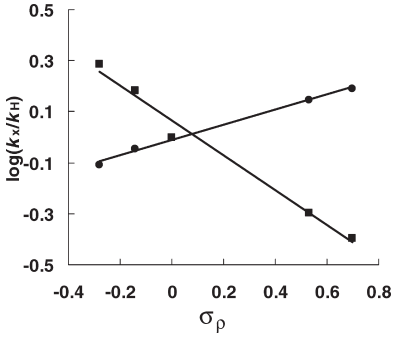

Figure 2. Hammett plots of the coupling reaction of *para*-substituted *p*-X-$C_6H_4CO_2H$ (X = OMe, CH_3, H, CF_3, CN) with phenylacetylene in $CDCl_3$ (●) and in THF (■).

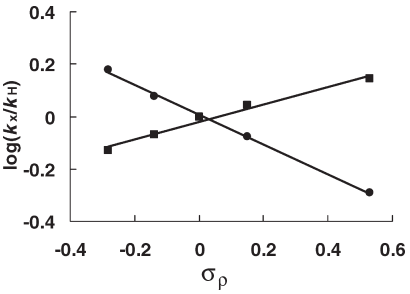

Figure 3. Hammett plots of the coupling reaction of benzoic acid with *para*-substituted *p*-Y-$C_6H_4C{\equiv}CH$ (Y = OMe, CH_3, H, F, CF_3) in $CDCl_3$ (●) and in THF (■).

In an effort to form a catalytically relevant ruthenium-vinylidene complex, the reaction of the ruthenium-carboxylate complex **6** with terminal alkynes was performed in THF. Thus, the treatment of complex **6** (44 mg, 0.050 mmol) with phenylacetylene (1.2 equiv) in THF at 95 °C for 10 h led to the coupling product **7**, which was isolated in 85% yield as a pale yellow-colored solid. The ^{1}H NMR of complex **7** showed a diagnostic vinyl peak at δ 6.24 (br s), and two distinct α-carbonyl peaks at δ 208.8 (t, J_{CP} = 14.4 Hz, Ru-CO) and 190.2 (t, J_{CP} = 12.1 Hz, Ru-*C*(O)CHPh) were also observed by the $^{13}C\{^1H\}$ NMR.

The molecular structure of **7** as determined by X-ray crystallography showed a syn orientation between the carboxylate oxygen atom and the phenyl group that apparently resulted from the coupling between the carboxylate and the vinylidene ligands (Figure 5). The structure clearly implicates the formation of the (*Z*)-enol ester product (*Z*)-**3k** from the protonation by another carboxylic acid. To show the enol ester product formation, the complex **7** was treated with an equivalent of benzoic acid in THF, which produced the carboxylate complex **6** and (*Z*)-**3k** along with another unidentified ruthenium complex upon heating at 90 °C for 2 h. Furthermore, the activity of both complexes **6** and **7** was found to be virtually identical to **1** for the coupling reaction of benzoic acid and phenylacetylene in THF (>90% yield with 2 mol % of **7**).

The successful isolation of the catalytically relevant complexes **6** and **7** enabled us to further examine the kinetics for the formation of these complexes. The treatment of **1** (14 mg, 0.020 mmol) with excess amounts of *p*-OMe-$C_6H_4CO_2H$ (10 equiv) and HC≡CPh (15 equiv) in THF was followed by ^{1}H and ^{31}P NMR (Scheme 2). As expected, the formation of the previously synthesized

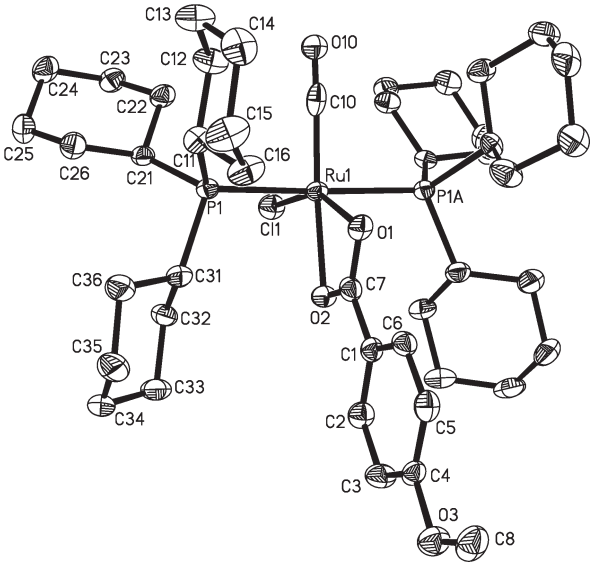

Figure 4. Molecular structure of **6**.

ruthenium-vinyl complex **8** was observed after 15 min at room temperature.[23] Upon warming to 40 °C, the vinyl complex **8** was slowly converted to the carboxylate complex **6** within 10 min along with the formation of styrene. At 60 °C, the signals due to the vinylidene-carboxylate complex **7** gradually appeared at the expense of the carboxylate complex **6**. Eventually, the formation of the coupling product (*Z*)-**3k** along with

Scheme 2

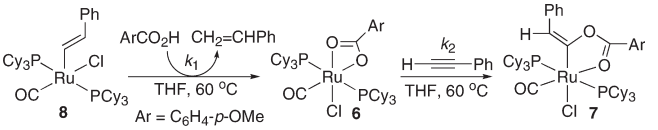

$Cy_3PH^+PhCO_2^-$ was observed after heating at 90 °C for 2 h.

The kinetics of the conversion of the vinyl complex **8** to the vinylidene-carboxylate complex **7** was followed by ^{31}P NMR (Figure 6). In a J-Young NMR tube, **1** (14 mg, 0.020 mmol), 4-methoxybenzoic acid (30 mg, 0.20 mmol), and phenylacetylene (31 mg, 0.30 mmol) were dissolved in THF (0.5 mL). The formation of the vinyl complex **8** was completed within 10 min at room temperature. The appearance of **6** and **7** was monitored by ^{31}P NMR at 60 °C in 5 min intervals. The experimental data were successfully fitted to the kinetic equation for two consecutive reaction kinetics by using nonlinear regression techniques for the conversion of **8** to **7** (Sigmaplot Version 10).[24] The rate constants $k_1 = 0.039\ min^{-1}$ and $k_2 = 0.013\ min^{-1}$ were obtained from this analysis. A relatively smaller value of k_2 compared to k_1 is consistent with the rate-limiting C−O bond formation step.

Proposed Mechanism. We propose a mechanism of the coupling reaction involving a coordinatively unsaturated ruthenium-carboxylate complex **9** as one of the key intermediate species (Scheme 3). The phosphine inhibition study suggests that the catalytically active 16 e^- complex **9** is formed from the Ru-carboxylate complex **6** by a reversible phosphine dissociation. For the coupling reaction in a noncoordinating solvent such as CH_2Cl_2, the direct migratory insertion of the

(23) (a) Yi, C. S.; Lee, D. W.; Chen, Y. *Organometallics* **1999**, *18*, 2043–2045. (b) Yi, C. S.; Lee, D. W. *Organometallics* **1999**, *18*, 5152–5156.

(24) See Supporting Information for the derivation of the kinetic equation.

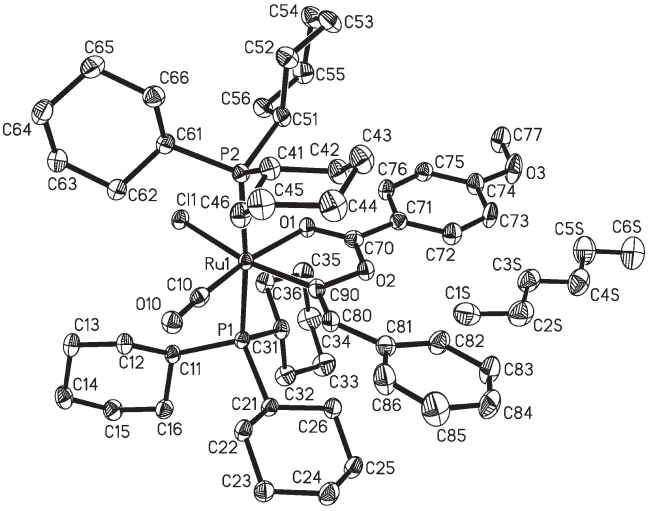

Figure 5. Molecular structure of **7**.

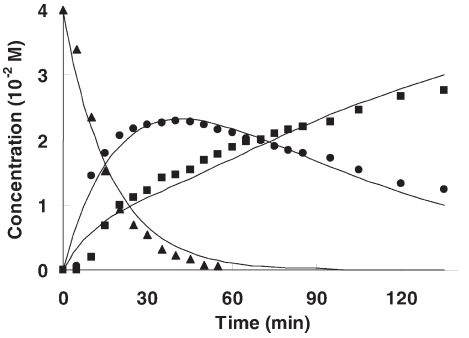

Figure 6. Kinetic profile of the conversion of **8** to **7**. Notations: **8** (▲), **6** (●), **7** (■).

carboxylate oxygen to the internal carbon of the alkyne substrate would be preferred over the terminal one to give the *gem*-enol ester product **2**. The dative coordination of the carboxylic oxygen atom would also promote the insertion by stabilizing intermediate species. On the other hand, the formation of (*Z*)-enol ester product (*Z*)-**3** is rationalized by invoking the formation of Ru-vinylidene species **10**. It has been well-established that the acetylene-to-vinylidene rearrangement is relatively facile for aryl-substituted alkynes.[10,21] The ability to promote the acetylene-to-vinylidene rearrangement for the ruthenium catalyst should be an important factor for the stereoselective formation of (*Z*)-enol ester products, and the coordinating solvent THF would facilitate such rearrangement by stabilizing a coordinatively unsaturated Ru-vinylidene species.

The Hammett study suggested that the C−O bond formation of the catalytic coupling reaction is strongly influenced by the electronic nature of the substrates. For the coupling reaction in CH_2Cl_2, this implies a direct migratory insertion of the coordinated terminal alkyne to the Ru-carboxylic oxygen bond, where both steric and electronic factors dictate the Markovnikov-selective formation of the *gem*-enol ester product **2**. The dative coordination of the carbonyl oxygen to the Ru center would also facilitate this transformation by avoiding the formation of a high-energy 14-electron species.

The successful isolation of **6** and **7** and their kinetic reaction profile provided new mechanistic insights for the formation of (*Z*)-enol ester product (*Z*)-**3**. The reversible dissociation of PCy_3 from both complexes **6** and **7** should form the catalytically active species for the coupling reaction,

Scheme 3. Proposed Mechanism of the Coupling Reaction of Carboxylic Acids and Terminal Alkynes

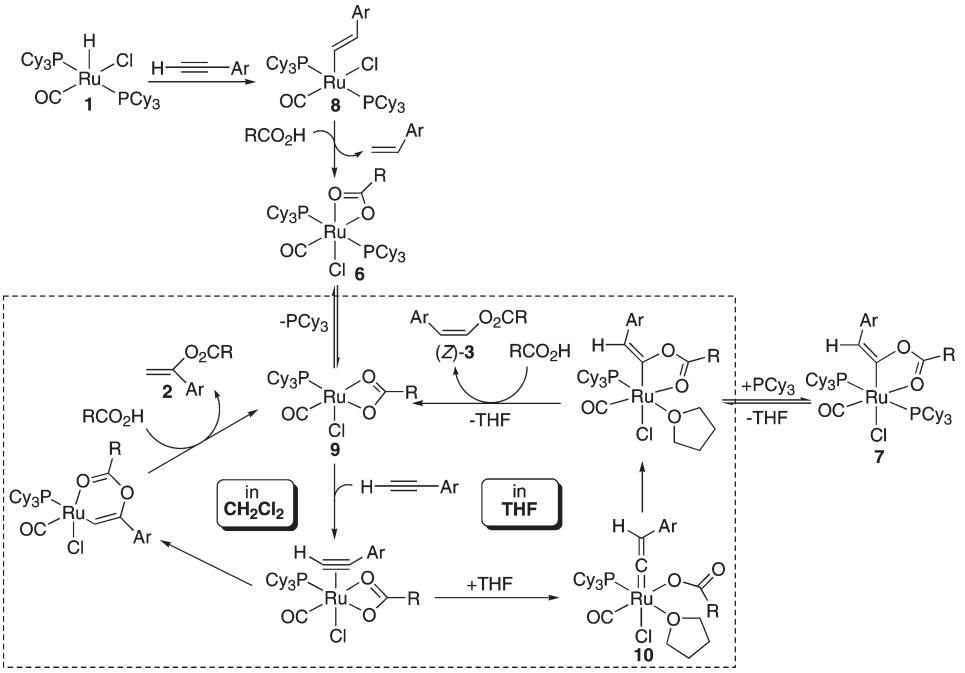

and in this regard, the formation of Cy_3PH^+ from the protonation of free PCy_3 by the carboxylic acid substrate would prohibit the recoordination of the phosphine ligand to the Ru center. The syn geometry of the vinylidene-carboxylate ligand of **7** clearly indicates that the formation of (*Z*)-enol ester product (*Z*)-**3** is electronically controlled during the addition of a carboxylate group to the α-vinylidene ligand of the ruthenium-vinylidene species **10**. Such cis addition of the carboxylate group could also be facilitated by the dative coordination of the carboxylate oxygen atom. A complementary computational study on the catalytic coupling reaction would be prudent in identifying these catalytically active intermediate species.

Concluding Remarks

The ruthenium-hydride complex **1** was found to be a highly effective catalyst for the alkyne-to-carboxylic acid coupling reaction to give synthetically valuable enol esters. Regio- and stereoselectivity of the catalyst **1** was successfully controlled by using CH_2Cl_2 and THF. From a synthetic point of view, the ruthenium catalyst **1** exhibited a number of salient features including its ability to control the activity and selectivity on the enol ester product formation with a relatively low catalyst loading, and a broad substrate scope under relatively moderate reaction conditions. The kinetic and mechanistic investigations as well as the successful isolation of Ru-carboxylate and -vinylidene-carboxylate complexes **6** and **7** provided a detailed mechanistic picture for the coupling reaction. The mechanistic knowledge gained from this study should give invaluable insights in designing the next generation of metal catalysts for the alkyne-to-carboxylic acid coupling reaction.

Experimental Section

General Information. All operations were carried out in a nitrogen-filled glovebox or by using standard high-vacuum and Schlenk techniques unless otherwise noted. Tetrahydrofuran, benzene, hexanes, and Et_2O were distilled from purple solutions of sodium and benzophenone immediately prior to use. The NMR solvents were dried from activated molecular sieves (4 Å). All carboxylic acid and alkyne substrates were received from commercial sources and used without further purification. $RuCl_3 \cdot 3H_2O$ and $Ru_3(CO)_{12}$ were obtained from commercial sources, and the complex **1** was prepared by following a reported procedure.[23] The ^1H, ^2H, ^{13}C, and ^{31}P NMR spectra were recorded on a Varian Mercury 300 or 400 MHz FT-NMR spectrometer. Mass spectra were recorded from a Agilent 6850 GC/MS spectrometer. The conversion of organic products was measured from a Hewlett-Packard HP 6890 GC spectrometer. Elemental analyses were performed at the Midwest Microlab, Indianapolis, IN.

General Procedure of the Catalytic Reaction. In a glovebox, a carboxylic acid (1.0 mmol), a terminal alkyne (2.0 mmol), and the ruthenium catalyst **1** (14 mg, 2 mol %) were dissolved in 3 mL of CH_2Cl_2 (or THF) in a 25 mL Schlenk tube equipped with a Teflon stopcock and a magnetic stirring bar. The reaction tube was brought out of the box and was stirred in an oil bath at 90−95 °C for 10−12 h. The tube was opened to air at room temperature, and the crude product mixture was analyzed by GC. An analytically pure organic product was isolated by a column chromatography on silica gel (hexanes/EtOAc). While we have not encountered any problems, the reaction in CH_2Cl_2 must be carried out with extra caution because of its relatively low boiling point. A thick-walled Schlenk tube with enough volume reservoir is strongly recommended.

Phosphine Inhibition Study. In a glovebox, benzoic acid (24 mg, 0.20 mmol), phenylacetylene (40 mg, 0.40 mmol), **1** (3 mg, 2 mol %), and C_6Me_6 (5 mg, internal standard) were dissolved in $CDCl_3$ (0.5 mL) in a J-Young NMR tube with a Teflon screw cap. A predissolved PCy_3 in $CDCl_3$ solution (5−15 μL, 10−30 mM) was added to the tube via syringe. The tube was brought out of the glovebox and was heated in an oil bath at 95 °C. The reaction was monitored by ^1H NMR in 30 min intervals. The rate was measured by the ^1H integration of the product peak at δ 5.61 (=CH_2) and was normalized against the internal standard peak. The k_{obs} was estimated from the first-order plot of *ln*[product] vs reaction time.

Isotope Labeling Study. In a glovebox, benzoic acid (122 mg, 1.0 mmol) and DC≡CPh (206 mg, 2.0 mmol) were added via syringe to a 25 mL Schlenk tube equipped with a magnetic

stirring bar and Teflon stopcock. The predissolved catalyst **1** (14 mg, 2 mol %) in CH_2Cl_2 or THF (3 mL) was added to the reaction tube. The reaction tube was brought out of the box and was stirred in an oil bath at 95 °C for 10 h. The solvent was removed from a rotary evaporator, and the organic product was isolated by column chromatography on silica gel (hexanes/CH_2Cl_2, 3:2). The deuterium content of the products **2c** and **3c** was measured from both ^{1}H NMR ($CDCl_3$ with 10 mg of cyclohexane as the external standard) and ^{2}H NMR (CH_2Cl_2 with 50 μL of $CDCl_3$).

Hammett Study: Reaction in $CDCl_3$. In a glovebox, a *para*-substituted acid *p*-X-$C_6H_4CO_2H$ (X = OMe, CH_3, H, CF_3, CN) (0.20 mmol), phenylacetylene (40 mg, 0.40 mmol), **1** (3 mg, 2 mol %), and C_6Me_6 (5 mg, internal standard) were dissolved in $CDCl_3$ (0.5 mL) solution in a J-Young NMR tube with a Teflon screw cap. The tube was brought out of the glovebox and was heated in an oil bath set at 95 °C. The reaction was monitored by ^{1}H NMR in 10 min intervals. The k_{obs} was estimated from a first-order plot of *ln*[product] vs reaction time by measuring the ^{1}H integration of the product peak (=CH_2, δ 5.61 ppm), which was normalized against the internal standard peak.

Reaction in THF. In a 25 mL Schlenk tube equipped with a Teflon stopcock and a magnetic stirring bar, a *para*-substituted acid *p*-X-$C_6H_4CO_2H$ (X = OMe, CH_3, H, CF_3, CN) (1.0 mmol), phenylacetylene (200 mg, 2.0 mmol), **1** (14 mg, 2 mol %), and C_6Me_6 (26 mg, internal standard) were dissolved in THF (3 mL) in a glovebox. The tube was brought out of the glovebox and was heated in an oil bath at 95 °C. The reaction was monitored by GC in 10 min intervals. The k_{obs} was estimated from a first-order plot of *ln*[product] vs reaction time by measuring the amount of the products against the internal standard.

Kinetic Profile Experiment. In a glovebox, **1** (14 mg, 0.02 mmol), 4-methoxybenzoic acid (30 mg, 0.20 mmol), and HC≡CPh (31 mg, 0.30 mmol) were dissolved in THF (0.5 mL) in a J-Young NMR tube with a Teflon screw cap. The tube was brought out of the glovebox and was placed in NMR probe, which was preset at 60 °C. The appearance and disappearance of the phosphine signals for **8** (δ 24.4), **6** (δ 25.9), and **7** (δ 23.4) were monitored by ^{31}P NMR at 60 °C in 5 min intervals. The rate of the product formation was determined by measuring the integration of the product peaks against the disappearance of the complex **8**. By using a nonlinear regression technique (Sigmaplot Version 10), the experimental data were globally fitted to the kinetic equation as shown in Figure 6. The rate constants $k_1 = 0.039\ min^{-1}$ and $k_2 = 0.013\ min^{-1}$ were obtained from this analysis.

Synthesis of $(PCy_3)_2(CO)(Cl)Ru(\kappa^2\text{-}O_2CC_6H_4\text{-}p\text{-}OMe)$ (6). In a glovebox, 4-methoxybenzoic acid (13 mg, 0.10 mmol), phenylacetylene (10 mg, 0.10 mmol), and complex **1** (73 mg, 0.10 mmol) were dissolved in CH_2Cl_2 (3 mL) in a 25 mL Schlenk tube equipped with a Teflon screw cap stopcock and a magnetic stirring bar. The tube was brought out of the box and was stirred at room temperature for 10 h. The solvent was evaporated, and the residue was washed with hexanes (3 mL × 3 times) to obtain **6** in 87% yield. Single crystals suitable for X-ray crystallographic study were obtained from hexanes/CH_2Cl_2.

For **6**: ^{1}H NMR (400 MHz, $CDCl_3$) δ 7.88 (d, J = 8.7 Hz, Ph), 6.89 (d, J = 8.7 Hz, Ph), 3.86 (s, OCH_3), 2.30−1.01 (m, PCy_3); $^{13}C\{^1H\}$ NMR (100 MHz, $CDCl_3$) δ 208.8 (t, J_{CP} = 13.3 Hz, CO), 179.0 (s, CO_2), 162.9, 130.3, 125.1, and 113.6 (C_{Ar}), 55.5 (OCH_3), 34.1, 30.2, 29.7, 28.3, and 26.8 (PCy_3); $^{31}P\{^1H\}$ NMR (161 MHz, $CDCl_3$) δ 28.7 (s, PCy_3); IR (KBr) ν_{CO} 1913 cm^{-1}.

Synthesis of $(PCy_3)_2(CO)(Cl)RuC(=CHPh)O_2CC_6H_4\text{-}p\text{-}OMe$ (7). In a glovebox, the Ru-carboxylate complex **6** (44 mg, 50 μmol) and phenylacetylene (6 mg, 60 μmol) were dissolved in THF (3 mL) in a 25 mL Schlenk tube equipped with a Teflon screw cap stopcock and a magnetic stirring bar. The tube was brought out of the glovebox and was heated in an oil bath at 95 °C for 10 h. The solvent was removed under high vacuum, and the residue was washed with hexanes (5 mL × 3 times) to obtain analytically pure **7** in 85% yield. Single crystals suitable for X-ray crystallographic study were obtained from hexanes/CH_2Cl_2.

For **7**: ^{1}H NMR (400 MHz, C_6D_6) δ 8.44 (d, J = 8.7 Hz, 2H, Ph), 7.76 (d, J = 7.7 Hz, 2H, Ph), 7.36−6.63 (m, Ar), 7.76 (d, J = 7.7 Hz, 2H, Ar), 7.36−6.63 (m, Ph); $^{13}C\{^1H\}$ NMR (100 MHz, $CDCl_3$) δ 209.8 (t, J_{PC} = 14.4 Hz, CO), 190.2 (t, J_{PC} = 12.2 Hz, Ru-*C*=CH), 173.8 (CO_2), 167.9, 165.4, 138.4, 133.8, 129.1, 125.0, 122.5, and 120.0 (C_{Ar}), 115.1 (=CH), 55.4 (OCH_3), 35.2, 31.1, 30.6, 29.8, 28.8, and 27.3 (PCy_3); $^{31}P\{^1H\}$ NMR (161 MHz, $CDCl_3$) δ 27.0 (s, PCy_3); IR (KBr) ν_{CO} 1922 cm^{-1}.

Acknowledgment. Financial support from the National Institute of Health, General Medical Sciences (R15 GM55987), is gratefully acknowledged. We also thank Dr. Sergey Lindeman (Marquette University) for X-ray crystallographic determination of the ruthenium complexes.

Supporting Information Available: Spectroscopic data of organic products and X-ray crystallographic data of **6** and **7**. This material is available free of charge via the Internet at http://pubs.acs.org.